Calculating vibrational excited state absorptions with excited state constrained minimized energy surfaces

Yiwen Wang, Zehua Chen, and Yang Yang*

Theoretical Chemistry Institute and Department of Chemistry, University of Wisconsin-Madison, 1101 University Avenue, Madison, Wisconsin 53706, United States

E-mail: yyang222@wisc.edu

Abstract

The modeling and interpretation of vibrational spectra are crucial for studying reaction dynamics using vibrational spectroscopy. Previous theoretical developments have mainly focused on fundamental vibrational transitions. In this study, we present a new method that uses excited state constrained minimized energy surfaces (CMES) to describe vibrational excited state absorptions. The excited state CMESs are obtained similarly to the previous ground state CMES development in our group but with additional wave function orthogonality constraints. Using a series of model systems, including the harmonic oscillator, Morse potential, double-well potential, and quartic potential, we demonstrate that this new procedure provides good estimations of the transition frequencies for vibrational excited state absorptions. The results are significantly better than those obtained from harmonic approximations using conventional potential energy surfaces.

Introduction

Vibrational spectroscopy has been a powerful tool to obtain structural information and uncover reaction dynamics in both gas and condensed phase[1–3]. Compared to conventional linear vibrational spectroscopy,[4] nonlinear vibrational spectroscopy[5,6] can additionally provide more information by probing two or more photon processes. For example, two-dimensional infrared spectroscopy (2DIR)[7] can go beyond the vibrational ground state and monitor the vibrational excited state dynamics and thus has been used to investigate reaction dynamics in a variety of materials and biological systems[8,9]

There have been many theoretical methods to model vibrational spectroscopy. A most widely used method to estimate vibrational frequencies is to diagonalize the mass-weighted Hessian matrices obtained from either density functional theory (DFT) or wave function theories. This method invokes the harmonic approximation and can generally provide qualitatively correct vibrational modes results; however, when describing systems with strong anharmonicities, it often needs to rely on empirical scaling factors to obtain quantitatively right results. Going beyond the harmonic approximation, vibrational second order perturbation theory (VPT2)[10–12] is often used to obtain anharmonicity-corrected vibrational frequencies, which utilizes information of local higher-order derivatives. VPT2 is currently considered to have reached a good balance between accuracy and efficiency, although it may face challenges when local higher-order derivatives are not sufficient to capture the behavior of the whole potential energy surface (PES), especially in some shared proton systems with double-well PESs. Vibrational self-consistent field theory (VSCF)[13,14] is currently one of the most accurate methods for obtaining vibrational spectra. It utilizes the high-dimensional PES to compute vibrational ground and excited states. However, due to the high computational cost of constructing the high-dimensitional PES, VSCF is often limited to small systems.

In addition to aforementioned popular methods based on static calculations, there is another category of methods that is based on dynamic simulations and employs time au-

tocorrelation functions to obtain vibrational spectra. Among them, a widely-used method is classical molecular dynamics (MD)[15–17], which treats nuclei as classical particles and let them evolve classically on PESs following Newton's laws of motion. Within the classical MD framework, *ab initio* MD (AIMD)[18] is generally more accurate than force-field-based MD because the PESs used in AIMD are obtained through *ab initio* electronic structure calculations, such as DFT. However, classical MD can only take into account limited amount of anharmonicty through dynamic simultations on PESs at a finite temperature and often needs empirical scaling factors for highly anharmonic systems. An improved way to incorporate more anharmonicity in MD simulations is through quasi- or semi- classical methods[19–22]. These methods assign certain initial energies to the nuclei, and thus the resulting classical trajectories can reach more anharmonic areas of the PES. This treatment is successful in many model systems and practical systems, although they can suffer from zero-point energy (ZPE) leakage problems[23–25] in some systems. A more elegant way of incorporating anharmonicity in MD simulations is through the path-integral formulism. A few major variants are centroid molecular dynamics (CMD)[26,27], ring-polymer molecular dynamics (RPMD)[28], thermostated ring-polymer molecular dynamics (TRPMD)[29], and quasi-centroid molecular dynamics (QCMD)[30]. They map a quantum nuclear system onto a classical system with chains of beads, and through a good description of the nuclear quantum effects as well as approximations on the autocorrelation functions, they can well describe the anharmonicity and give relatively accurate vibrational spectra. An even more accurate method to describe vibrational spectra is through quantum nuclear dynamics, and a commonly-used method is the multiconfigurational time-dependent Hartree (MCTDH)[31] theory. This theory has been shown to accurately describe the vibrational spectra of systems as large as water clusters with four water molecules, although the underlying computational cost remains a major limiting factor.

In the past few years, our group has developed a new method for calculating vibrational spectra based on constrained minimized energy surfaces (CMESs)[32]. The CMES is an effec-

tive PES for nuclei, but compared to the conventional PES, the CMES incorporates nuclear quantum effects, especially the zero-point effects, in the effective potential energy surface. It has been shown with a few model systems that MD based on the CMES (CMES-MD) is able to give significantly more accurate fundamental vibrational frequencies than conventional MD, and its performance is comparable to or even better than CMD and RPMD. In real molecular systems, our group has developed constrained nuclear-electronic orbital density functional theory (CNEO-DFT) to approximate the CMES. It was found that CNEO-DFT harmonic frequencies are already comparable to or better than VPT2[33–35], and the vibrational spectra obtained from MD simulations on CNEO-DFT energy surfaces accurately reproduce the experimental spectra[36]. Despite the great success, these past developments were mostly focused on the fundamental $0 \rightarrow 1$ excitations. In order to simulate non-linear vibrational spectra, especially the $1 \rightarrow 2$ excitations, a method that can describe vibrational excited state absorption is essential. One example is that in a 2D-IR spectrum, the $0 \rightarrow 1$ fundamental transitions show up on the diagonal line, whereas the $1 \rightarrow 2$ excited state absorptions can be observed next to them but slightly off the diagonal line, together forming the butterfly-shaped feature of the spectrum.

For the excited state absorptions, conventional MD cannot distinguish them from fundamental transitions since the underlying theoretical foundation for spectra calculations using MD is a harmonic approximation, in which the fundamental $0 \rightarrow 1$ excitation and all excited state $n \rightarrow n+1$ transitions share the same transition energy. Quasi- or semi- classical methods can possibly describe these excited state absorptions by giving more initial energy to the nuclei. However, their ZPE leakage problems could be more severe because of the even higher initial energy given to the systems. Currently, the commonly used method for describing the vibrational excited state absorptions in the 2DIR spectrum is to first obtain the PES for the mode of interest while fixing all other modes[37–41], and then either fit the PES to a Morse potential and approximate the results with the exact quantum solutions for the Morse potential, or utilize the discretized variable representation (DVR) method to solve the

Shrödinger equation on this one-mode PES. Both of these two ways can yield qualitatively correct results but the quantitative accuracy can be questionable due to the approximations made during the calculations. Therefore, it remains highly desirable to develop a method that can accurately and efficiently simulate vibrational excited state absorptions.

In this paper, we propose a new way of calculating vibrational excited state absorptions by constructing excited states CMESs and using their second-order derivative information to approximate the vibrational transition energies. This is essentially equivalent to performing MD simulations at the zero-temperature limit. We systematically test the new method on a series of 1-D model systems and benchmark against the exact quantum reference. We will show that the results are significantly better than the harmonic approximation results based on the ground state PES. This paper will serve as the theoretical foundation for our future development of using excited states CNEO theory to calculate vibrational excited state absorptions in real molecular systems.

The paper is organized in the following way: In section 2, we first review the theory of constructing ground state CMESs and provide our way of constructing excited state CMESs, then we provide a brief theoretical analysis on excited state CMES for the quantum harmonic oscillator model and show that our method is exact within the harmonic approximation. In section 3, we apply and numerically test the new theory on a series of model systems including Morse potential, quartic potential, and double-well potential systems. We give our concluding remarks in section 4.

Theory

Ground state CMES

Recently, our group developed a new framework of incorporating nuclear quantum effects in MD simulations through CMESs[32]. In conventional PES-based MD simulations, nuclei are treated as point charges that are highly localized in space. This treatment loses the quantum

delocalization picture for nuclei. In contrast, in CMES-MD, nuclei are treated quantum mechanically, but instead of directly evolving the quantum nuclei rigorously according to the time-dependent Schrödinger equation, we invoke an adiabatic assumption that every time the nuclei evolve to a quantum state with certain expectation positions and expectation momenta $(\mathbf{X}, \mathbf{P})$, the system always relaxes to the energy-minimized quantum state with the same $(\mathbf{X}, \mathbf{P})$. Under this assumption, it can be proved that the nuclear expectation positions and expectation momenta evolve classically according to the Newton's law of motion but with a caveat that nuclei evolve on the effective potential energy surface, i.e., the CMES, instead of the conventional PES.

A key to performing CMES-MD is to construct the CMES, which is a function of nuclear expectation positions and can be obtained by searching for the lowest-energy nuclear wave function that satisfies the nuclear expectation position constraint:

$$V_0^{\mathrm{CMES}}(\mathbf{X}) = \min_{A_0 \in \{A \in \mathscr{H} | \langle A|\hat{\boldsymbol{x}}|A\rangle = \mathbf{X}\}} \langle A_0|\hat{H}|A_0\rangle \tag{1}$$

Here $\mathscr{H}$ is the quantum nuclear Hilbert space and the nuclear expectation constraint is $\langle A|\hat{\boldsymbol{x}}|A\rangle = \mathbf{X}$. This constrained minimization can be performed using the Lagrangian function:

$$\mathcal{L} = \langle A_0|\hat{H}|A_0\rangle + \boldsymbol{f}_0 \cdot (\langle A_0|\hat{\boldsymbol{x}}|A_0\rangle - \mathbf{X}) - \tilde{E}_0(\langle A_0|A_0\rangle - 1) \tag{2}$$

in which $\boldsymbol{f}_0$ is the Lagrange multiplier associated with the expectation position constraint, and $\tilde{E}_0$ is the Lagrange multiplier associated with the wave function normalization constraint. Making the Lagrangian function stationary by varying the state $|A_0\rangle$ leads to an eigenvalue equation

$$[\hat{H} + \boldsymbol{f}_0 \cdot \hat{\boldsymbol{x}}]|A_0\rangle = \tilde{E}_0|A_0\rangle. \tag{3}$$

This eigenvalue equation can be solved iteratively together with the expectation constraint as well as the normalization constraint, leading to solutions of $\boldsymbol{f}_0$, $|A_0\rangle$, and $\tilde{E}_0$. When the constraints are satisfied, the total energy, which is a function of the nuclear expectation positions, will serve as the effective PES, or the CMES:

$$V_0^{\mathrm{CMES}}(\mathbf{X}) = \langle A_0|\hat{H}|A_0\rangle = \tilde{E}_0(\mathbf{X}) - \boldsymbol{f}_0(\mathbf{X}) \cdot \mathbf{X} \tag{4}$$

The nuclear expectation positions and momenta evolve according to the Newtonian equations

$$\begin{cases} \frac{\mathrm{d}\langle\hat{\boldsymbol{x}}\rangle}{dt} = & \frac{\langle\hat{\boldsymbol{p}}\rangle}{m} \\ \frac{\mathrm{d}\langle\hat{\boldsymbol{p}}\rangle}{dt} \approx & -\nabla_{\mathbf{X}} V_0^{\mathrm{CMES}}(\mathbf{X}) \end{cases} \tag{5}$$

Note again the evolution of momenta is not exact since we have invoked the adiabatic approximation and assumed the system always relaxes to the energy-minimized quantum state for a given nuclear expectation position $\mathbf{X}$.

Based on trajectories obtained from CMES-MD, our group showed that accurate vibrational spectra can be obtained in both model systems and practical molecular systems.

The theoretical justifications for these vibrational spectra simulation based on classical MD simulations, including both conventional MD and CMES-MD, is that 1. according to the Fermi's Golden Rule, the Fourier spectrum of quantum autocorrelation functions can be used to calculate transitional frequencies and intensities between energy levels [42], and 2. the classical autocorrelation functions and the quantum autocorrelation functions match exactly in peak positions and differ only by a universal factor in intensities in the harmonic oscillator model. Although this harmonic approximation justifies the use of classical MD simulations to calculate vibrational spectra, it also leads to the assumption that the fundamental excitations ($0 \rightarrow 1$) are the same in energy as those excited states absorptions (e.g. $1 \rightarrow 2$, $2 \rightarrow 3$). However, in anharmonic systems, there are slight differences among them, which can be observed, for example, in 2DIR experiments. We note that although it might be considered

that increasing the simulation temperature in MD simulations incorporates some excited states absorptions, there is no solid theoretical foundation for this temperature effect, and it is more of an artifact from classical treatments.

Excited states CMES

Here we propose a new way of separately obtaining excited states and ground state absorption frequencies by constructing and using excited-state CMESs.

Previously in developing the CMES theory, our group has been targeting on the eigenstate with the lowest energy. These states are essentially the ground states that satisfy the expectation constraints. However, there are also "excited states" with higher energies. To search for these excited states for a given nuclear expectation position, we can perform constrained energy minimization again. The first excited state can be defined as

$$V_1^{\mathrm{CMES}}(\mathbf{X}) = \min_{A_1 \in \{A \in \mathscr{H} | \langle A|\hat{\boldsymbol{x}}|A\rangle = \mathbf{X}, \langle A|A_0\rangle = 0\}} \langle A_1|\hat{H}|A_1\rangle, \tag{6}$$

in which we require the state to be orthogonal to the ground state in addition to the expectation position constraint. A more general definition for the nth excited state CMES surface can be defined as

$$V_n^{\mathrm{CMES}}(\mathbf{X}) = \min_{A_n \in \{A \in \mathscr{H} | \langle A|\hat{\boldsymbol{x}}|A\rangle = \mathbf{X}, \langle A|A_i\rangle = 0, \forall i = 0,1,\cdots,n-1\}} \langle A_n|\hat{H}|A_n\rangle \tag{7}$$

Note that here we require the nth excited constrained minimized energy state to be orthogonal with all the lower states with the same $\langle\hat{\boldsymbol{x}}\rangle$. Under these constraints, the Lagrangian function for excited states CMES can be written as

$$\mathcal{L} = \langle A_n|\hat{H}|A_n\rangle + \boldsymbol{f}_n \cdot (\langle A_n|\hat{\boldsymbol{x}}|A_n\rangle - \langle\hat{\boldsymbol{x}}\rangle) + \sum_{i=0}^{n-1} g_{ni} \cdot \left|\langle A_n|A_i\rangle\right|^2 - \tilde{E}_n(\langle A_n|A_n\rangle - 1), \tag{8}$$

where g_{ni} is the Lagrange multiplier associated with the orthogonality constraint with the

CMES state A_i. Here, to facilitate derivations and practical implementations next, we employ the constraint as $\left|\langle A_n|A_i\rangle\right|^2 = 0$ instead of the simple form of $\langle A_n|A_i\rangle = 0$. Making the Lagrangian function stationary by varying A_n can lead to the eigenvalue equation for solving the nth excited CMES state:

$$\left(\hat{H} + \boldsymbol{f}_n \cdot \hat{\boldsymbol{x}} + \sum_{i=0}^{n-1} g_{ni} \cdot |A_i\rangle\langle A_i|\right) |A_n\rangle = \tilde{E}_n |A_n\rangle. \tag{9}$$

With all lower states A_i known, this eigenvalue equation can be solved iteratively together with the expectation constraint, the normalization constraint, and the orthogonality constraints, which will give solutions of $\boldsymbol{f}_n$, g_{ni}, $|A_n\rangle$, and $\tilde{E}_n$. When all constraints are satisfied, the total energy will serve as the effective PES for the nth excited constrained minimized energy state:

$$V_n^{\mathrm{CMES}}(\mathbf{X}) = \langle A_n|\hat{H}|A_n\rangle = \tilde{E}_n(\mathbf{X}) - \boldsymbol{f}_n(\mathbf{X}) \cdot \mathbf{X} \tag{10}$$

These excited state CMESs can be used in an *ad hoc* manner to perform MD simulations. The underlying assumption for these simulations is that the nuclear wave functions adiabatically keep their excited state character during the dynamics and do not relax to the lower vibrational states. In the next section we will show that we can use them to obtain vibrational excited state absorption frequencies. For these frequency calculations, a natural question is that since we need to construct excited state CMESs, why not we directly take the energy difference between CMESs to obtain the frequencies? We note that because of the requirement on the orthogonality with the lower states of the same expectation position, the "excited states" for CMESs do not rigorously correspond to the vibrational excited states solved from the Schrödinger equation, therefore, the energy gaps between CMESs do not necessarily match well with the reference excited state absorption values. Additionally, intensity information will be more directly available from dynamics simulations than pure static energy calculation. Furthermore, the success of vibrational frequency calculations will

demonstrate the good quality, at least near the equilibrium region, of the vibrational excited state CMESs, which we can use in the future to perform excited state dynamics simulations.

Excited state CMES for harmonic oscillator model

The harmonic oscillator model was used to justify the use of classical MD to calculate vibrational spectra since its classical autocorrelation functions match exactly with the quantum autocorrelation functions in peak positions. Our group also showed that in the harmonic oscillator model, the ground state CMES differs from the underlying PES only by a universal shift of $\frac{1}{2}\hbar\omega$. Therefore, the classical dynamics picture remains the same, and CMES-MD is also exact for the harmonic oscillator. Here, to extend out CMES theory to excited states, we will analytically solve for the excited state CMESs for a harmonic oscillator and investigate their properties.

From a previous paper by our group,[32] the ground constrained minimized energy state $|A_0\rangle$ for the the harmonic oscillator model $\hat{H} = \hat{p}^2/2m + m\omega^2(x - x_e)^2/2$ is the ground state of another harmonic oscillator with the center shifted to the nuclear expectation position X. And the corresponding ground CMES is

$$V_0^{\mathrm{CMES}}(X) = \langle A_0|\hat{H}|A_0\rangle = \frac{1}{2}\hbar\omega + \frac{1}{2}m\omega^2(X - x_e)^2, \tag{11}$$

which is a function of X.

Now, we can substitute the ground CMES state $|A_0\rangle$ into Eq. 9 to solve the first excited CMES state analytically (see Supporting Information for details). The wave function $A_1(x; X)$ is

$$A_1(x; X) = \psi_1^{\mathrm{HO}}(x - X), \tag{12}$$

where $\psi_n^{\mathrm{HO}}(x)$ is the nth eigenfunction of a harmonic oscillator, and the corresponding CMES is

$$V_1^{\mathrm{CMES}}(X) = \langle A_1|\hat{H}|A_1\rangle = \frac{3}{2}\hbar\omega + \frac{1}{2}m\omega^2(X - x_e)^2. \tag{13}$$

It can be observed that the wave function is the same as the first excited state wave function for quantum harmonic oscillator except it is now centered at $x = X$. The excited state CMES is the same as the underlying harmonic PES except that it is here shifted up universally by $\frac{3}{2}\hbar\omega$, which is the quantum energy associated with the first excited state.

In fact, for the harmonic oscillator model, these elegant results can be generalized to even higher excited state CMESs with

$$V_n^{\text{CMES}} = \langle A_n|\hat{H}|A_n\rangle = (n + \frac{1}{2})\hbar\omega + \frac{1}{2}m\omega^2(X - x_e)^2, \tag{14}$$

which means that compared to the underlying harmonic PES, CMESs simply shift the energy universally up by $(n + 1/2)\hbar\omega$, which is the quantum energy for the nth state.

This universal shift does not change the shape of the effective potential and also does not change the classical dynamics picture. Therefore, the position autocorrelation functions remain the same for every excited state CMES:[42]:

$$\langle x(0)x(t)\rangle_n^{\text{CMES}} = \frac{kT}{m\omega^2}\cos\omega t, \tag{15}$$

where the average $\langle\cdot\rangle$ is taken under the canonical ensemble. Furthermore, the Fourier transform of this autocorrelation function gives the same vibrational frequency ω as before. Despite the same frequency, we argue that because these dynamics simulations are performed on excited CMESs and the underlying quantum picture corresponds to excited state harmonic oscillator wave functions, these vibrational frequencies ω should not be viewed as the fundamental transition frequency. Instead, they should be viewed as excited states absorption frequencies, which happen to be the same as the fundamental transition frequency in the harmonic oscillator model. This is the key hypothesis of this paper, which we will provide numerical support in Section 3 on a series of anharmonic model systems.

To further connect the classical autocorrelation functions with the quantum autocorrelation functions for excited states absorptions, here we consider a special ensemble for the

harmonic oscillator, in which the ground state is not occupied whereas the excited state are occupied according to the Boltzmann distribution. In this special ensemble, since the ground state is not occupied, the quantum autocorrelation function contains information of excited states absorptions (mainly $1 \rightarrow 2$) but no fundamental transition. The position autocorrelation function can be computed analytically:

$$\frac{1}{2}\langle\left[\hat{x}(0), \hat{x}(t)\right]_+\rangle = \frac{\hbar}{2m\omega}\frac{3 - e^{-\beta\hbar\omega}}{1 - e^{-\beta\hbar\omega}}\cos\omega t. \tag{16}$$

Obviously the Fourier transform of this quantum autocorrelation function still gives the frequency ω, but it should mainly be considered to correspond to the $1 \rightarrow 2$ transition. By comparing this quantum autocorrelation function with the classical autocorrelation function obtained from excited state CMES in Eq. 15, we only see a difference by a pre-factor, suggesting that it may be viable to use excited state CMES-MD to obtain excited state absorption spectra.

This argument can also be generalized to the $2 \rightarrow 3$ or even higher transitions by constructing other special ensembles, but the key hypothesis remains the same: since the classical autocorrelation function matches with the quantum autocorrelation function, we may use excited CMES-MD to obtain excited-state spectra.

Results for anharmonic systems

To go beyond the simple harmonic oscillator model, here we test our proposed method on a series of anharmonic model systems. Note that conventional MD has only one PES and cannot construct vibrational excited state surface. Therefore, we can only obtain the same frequency for both $0 \rightarrow 1$ fundamental transition and other $n \rightarrow n + 1$ excited states transitions. In contrast, in the CMES-MD framework, we can use MD on the ground state CMES to obtain $0 \rightarrow 1$ transition frequencies, use MD on the first excited CMES to obtain $1 \rightarrow 2$ transitions, and so forth. We note that although MD results depend on the simulation

temperature, this temperature effect is relatively small in the temperature range that most chemists care about. Therefore, in this paper, we will simply focus on the zero-temperature limit and only use their second-order derivative information to approximate the vibrational transition energies. We will provide results for the Morse potential, the quartic potential, and the double-well potential, all of which are important model systems for modeling practical chemical problems. The quantum results are used as reference, which are obtained either analytically or numerically with a dense grid.

Morse potential

The Morse potential is a typical model for bond vibrations. It has analytic quantum solutions, and the anharmonicity makes excited states transitions different from the $0 \rightarrow 1$ fundamental transition. Here we will test our method on the 1-D Morse potential with the form $V(x) = D_e(e^{-2\alpha(x-x_e)} - 2e^{-\alpha(x-x_e)})$, in which $D_e = hc\omega_e\chi_e^2/(4\omega_e\chi_e)$ and $\alpha = \sqrt{2\mu hc\omega_e\chi_e}/\hbar$. Three parameters, x_e, χ_e, and ω_e completely determine the Morse potential, but we will not scan all these parameters due to the large computational expense. Instead, we select a few parameter sets that mimic real chemical bond vibrations for testing.

The first group of bonds is H-X bonds, where X typically can be C, N, and O. This group of bonds is of particular interest because they are known to be highly anharmonic. In existing literatures[43], there have been Morse parameters sets fitted for these H-X bonds based on diatomic results, although we note that the bond strengths, bond lengths, and vibrational frequencies can vary with chemical environments and so do these parameters sets. We notice that in the existing Morse potential parameters sets, different H-X diatomic molecules tend to have similar χ_e and x_e values, but their ω_e can vary more. Therefore, we fix the value of χ_e to be 0.023 and the value of x_e to be 1.0Å, and only scan the value of ω_e in the range from 2000 cm^{-1} to 4000 cm^{-1} to model the H-X vibrations in different chemical environments. The reduced mass is approximated to be the mass of a hydrogen atom. We limit our discussions to $0 \rightarrow 1$, $1 \rightarrow 2$, and $2 \rightarrow 3$ transitions since the lowest

few states are more important. Therefore, we construct the ground, the first excited, and the second excited CMESs using the Eq. 3 and Eq. 9. Since we are focusing on the zero-temperature limit, we numerically obtain the second-order derivatives around the minima of each CMES to approximate the vibrational frequencies with harmonic approximation. We will use the exact analytic quantum results as references, and additionally we will also compare with harmonic approximation results from the PES, which are nothing but ω_e for Morse potentials.

Figure 1 shows the ground state, first excited state, and second excited state CMESs for $\omega_e = 3500\text{cm}^{-1}$. In addition to the relative energy difference, we also note that their energy minima correspond to different nuclear positions, which essentially indicates that the bond length will grow as the system is excited. Furthermore, these energy curves do not differ by a universal shift any more and thus will give different vibrational frequencies.

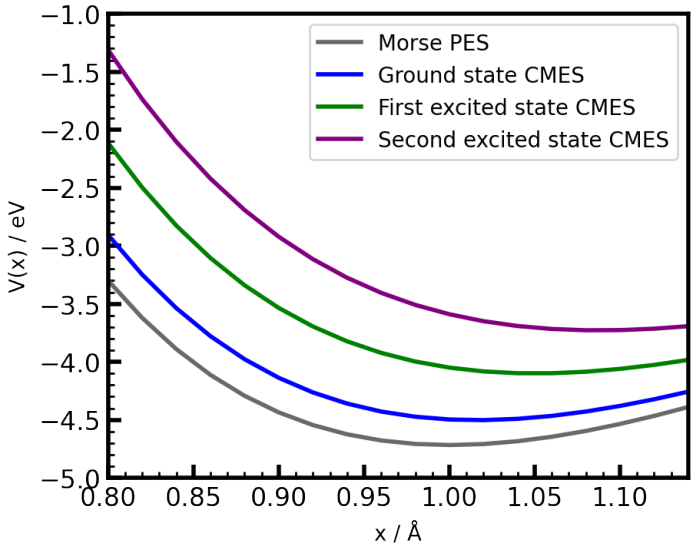

Figure 1: PES and ground and excited state CMESs for a 1D Morse potential. The parameters of the Morse potential are $\chi_e = 0.023$, $x_e = 1.0\text{Å}$, and $\omega_e = 3500\text{cm}^{-1}$

Figure 2 shows the CMES results for estimating $0 \to 1$, $1 \to 2$, and $2 \to 3$ transition frequencies. For the $0 \to 1$ fundamental frequencies (panel a), CMES harmonic approximation results excellently agree with the quantum reference results, with a percentage error of about 1%, whereas using the PES, the error is about 5%. These results are consistent with

results from the previous paper by two of us, where we found CMES-MD can significantly outperform conventional MD in predicting fundamental frequencies. For $1 \rightarrow 2$ transitions (panel b), the excited state CMES gives lower vibrational frequencies than those obtained from the ground state CMES. This trend is in great agreement with the quantum reference results, where $1 \rightarrow 2$ energy gap is smaller than the $0 \rightarrow 1$ energy gap due to anharmonicity. The percentage error is about 2% and slightly larger than that for the $0 \rightarrow 1$ fundamental transition. In contrast, the harmonic approximation based on the PES gives the same vibrational frequencies as the fundamental transitions and deviate more severely from the quantum reference. The story for $2 \rightarrow 3$ transitions (panel c) is highly similar: although the harmonic approximation based on CMES gives an larger percentage error (around 5%) than in the $0 \rightarrow 1$ and $1 \rightarrow 2$ cases, it captures the decreasing trend of the energy gap and significantly outperforms the harmonic approximation results based on the original PES.

To further investigate the performance of our method in more general bond stretch cases, we next choose the Morse potential parameters sets for the diatomic F-F, O=O and N≡N molecules. These three diatomic molecules can be good representatives of bond stretches for single bond, double bond, and triple bond respectively. The parameters used are taken from reference and are listed in Table S1 of the Supporting Information. The results for these systems are shown in Figure 3. We again see that our CMES-based method significantly outperforms the conventional PES-based method and for all $0 \rightarrow 1$, $1 \rightarrow 2$, and $2 \rightarrow 3$ transitions.

Double-well and quartic potential

Next we apply our method to the more challenging double-well and quartic potential systems, which both share the potential form of $V(x) = ax^2 + bx^4$. The parameter b is always positive. When a is negative, the potential corresponds to a double-well potential; when a is zero, there is no second order term and the potential is quartic; and when a is positive, it is a symmetric single well potential with anharmonicity coming from the quartic bx^4 term.

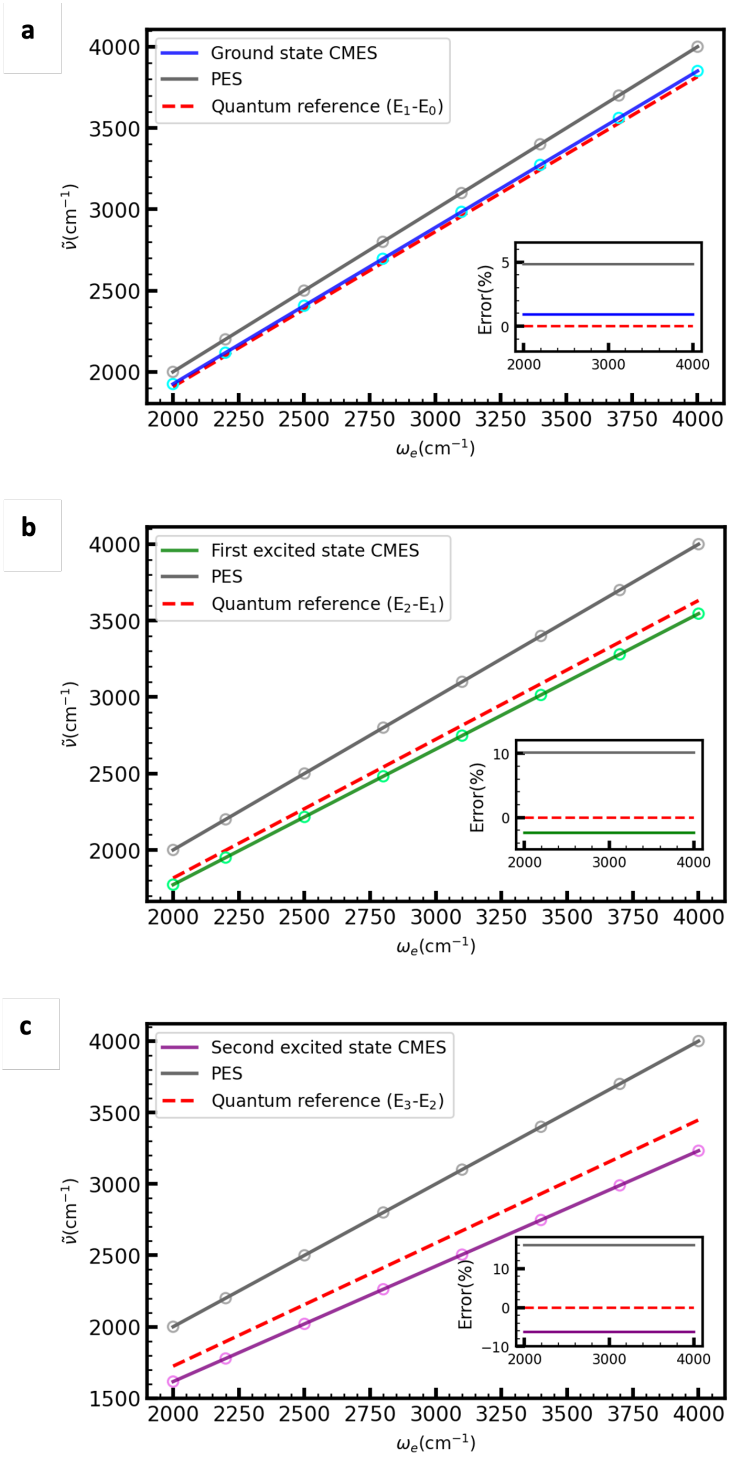

Figure 2: Transition frequencies from harmonic approximation using CMES (colored solid line) and PES (grey solid line) for (**a**) the fundamental frequencies (the $0 \rightarrow 1$ transition); (**b**) the $1 \rightarrow 2$ transition; and (**c**) the $2 \rightarrow 3$ transition. The red dashed lines are the exact quantum references. Based on the harmonic approximation, our CMES-based method greatly outperforms the conventional PES-based method.

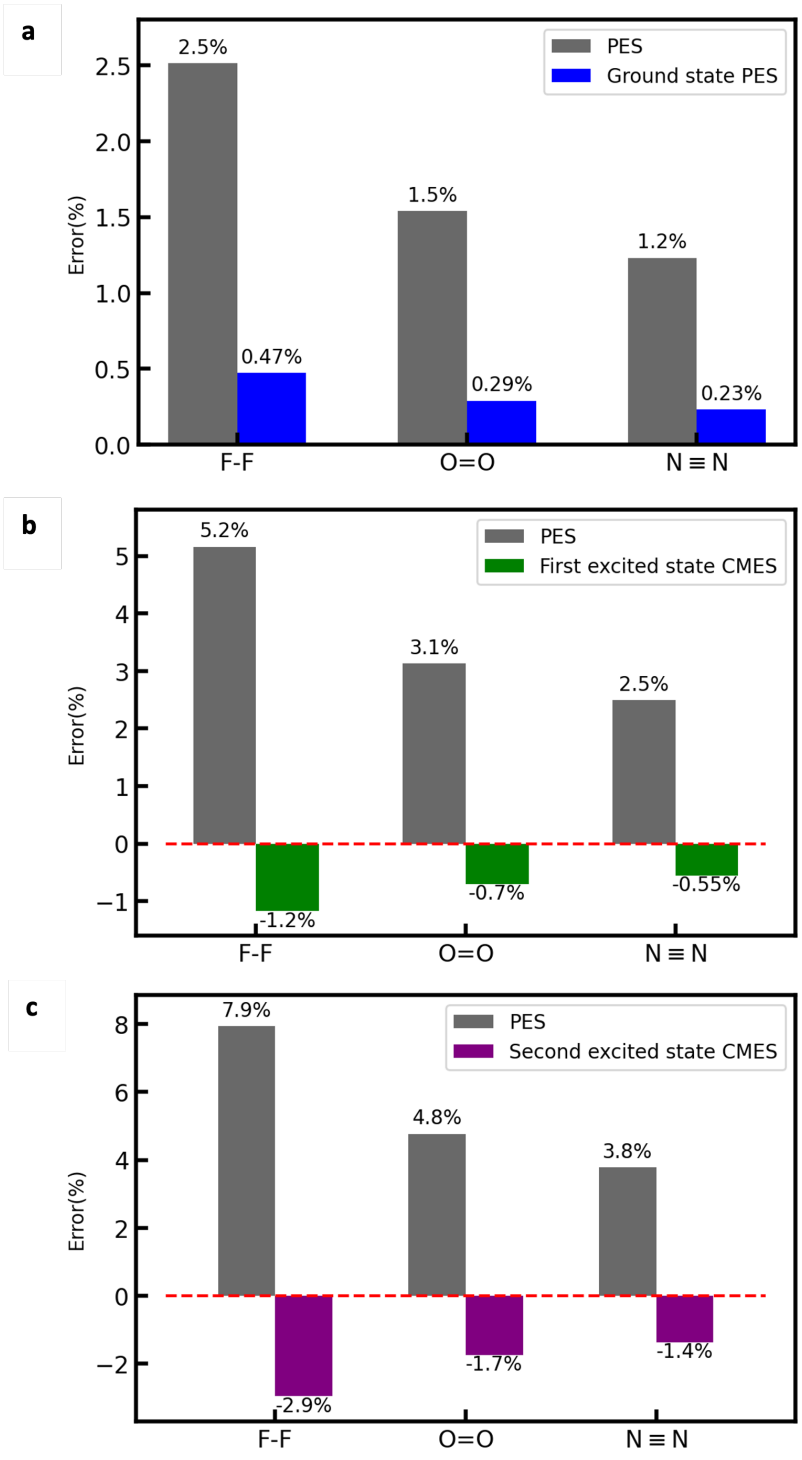

Figure 3: Relative percentage error between the calculated transition frequencies and the quantum references of F−F, O=O, N≡N bonds for (**a**) the fundamental frequencies (the $0 \rightarrow 1$ transition); (**b**) the $1 \rightarrow 2$ transition; and (**c**) the $2 \rightarrow 3$ transition. Results using CMESs are colored and results using PES are in grey. Our CMES-based method greatly outperforms the conventional method with much smaller percentage error.

Figure 4 shows the ground and the first excited state CMESs for these three scenarios. For quantitative testing, we fix the value of b to be $32\text{eV}/\text{Å}^4$ and vary a from $-8\text{eV}/\text{Å}^2$ to $12\text{eV}/\text{Å}^2$. The results for $0 \to 1$ and $1 \to 2$ transitions are shown in Figure 5, panel (a) and (b), respectively.

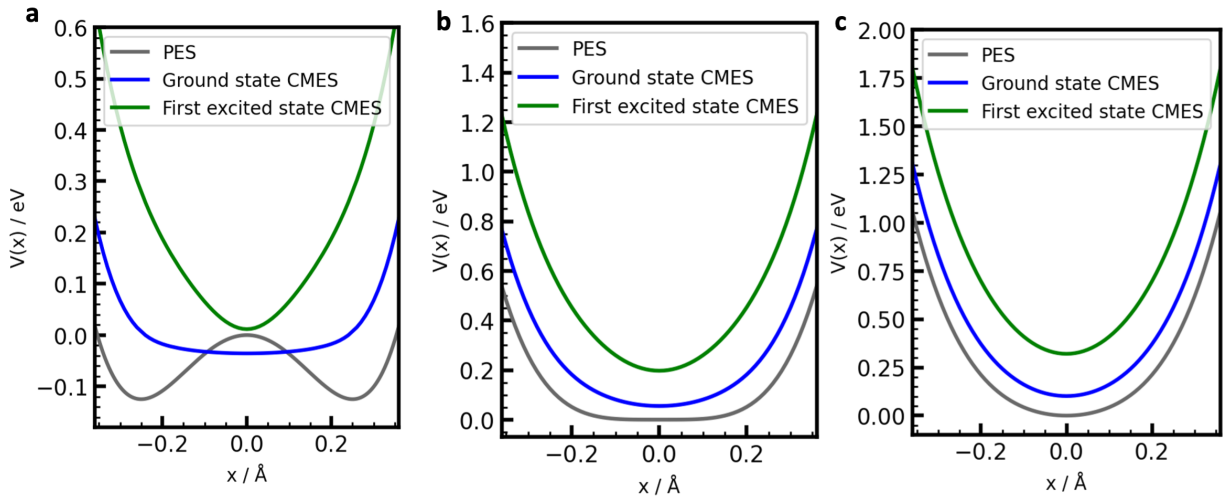

Figure 4: PES, ground state CMES, and first excited state CMES for model potential $V(x) = ax^2 + bx^4$. The parameter a varies with (**a**) $a = -4\text{eV}/\text{Å}^2$; (**b**) $a = 0\text{eV}/\text{Å}^2$; and (**c**) $a = 4\text{eV}/\text{Å}^2$. The parameter b are all set to be $32\text{eV}/\text{Å}^4$.

In the double well region where a is negative, the barrier decreases as a becomes less negative, making the $0 \to 1$ tunnelling splitting increase as seen in the quantum reference. This trend can be accurately captured by the harmonic results based on the ground state CMES. In contrast, conventional classical treatment based on PES cannot describe tunneling, and at the zero-temperature limit, the particle always get trapped in either side of the well, leading to generally overestimated frequencies. Additionally, because of the wrong physical picture, the increasing trend is completely missed. For the $1 \to 2$ transition, the energy gap generally decreases as a becomes less negative but turns flat and starts to increase when it is about $-4\text{eV}/\text{Å}^4$. This qualitative picture can be captured by our method based on the first excited state CMES, although we note that the quantitative agreement is not completely satisfactory, especially when a is a very negative number, CMES-MD could overestimate the gap by 100%. For the conventional classical treatment, although quantitatively it seems that

it can slightly outperform CMES-MD in most of the double-well excited state region with the grey curve being closer to the red curve than the green curve, we note that it does not mean that conventional MD is better since its underlying trapped-particle picture is completely unphysical.

For quartic potential with a being zero, CMES results still have an excellent agreement with the quantum reference for the $0 \rightarrow 1$ transition. For the $1 \rightarrow 2$ transition, its quantitative error is significantly reduced compared to that in the double-well case. In contrast, since there is no harmonic term, the classical treatment with harmonic approximation gives a zero frequency result, which is unphysical.

For cases with a greater than zero, the potential is an anharmonic single well potential. In this case, both the $0 \rightarrow 1$ and $1 \rightarrow 2$ energy gaps increase as a increases. This relatively easy trend can be captured by both our CMESs-based method and the conventional PES-based method. However, our method outperforms the conventional method with a significantly better agreement with the quantum references. In the large a limit, the quartic terms can be ignored and the potential essentially becomes an harmonic oscillator. According to the discussions on harmonic oscillator, both $0 \rightarrow 1$ and $1 \rightarrow 2$ gaps converge to the same value and all methods give the same and correct asymptotic result.

Conclusion

In summary, we developed a procedure to calculate excited state CMESs and used them to obtain approximate vibrational excited state absorption frequencies. In the harmonic oscillator model, we showed that our CMES results are exact via analytical derivations. In the Morse potential model, our CMES-based method is highly accurate and significantly outperforms conventional PES-based harmonic approximation results. In the more challenging double-well potential and quartic potential, our method gives the right physical picture and outperforms the conventional method. These results suggest that excited state CMESs can

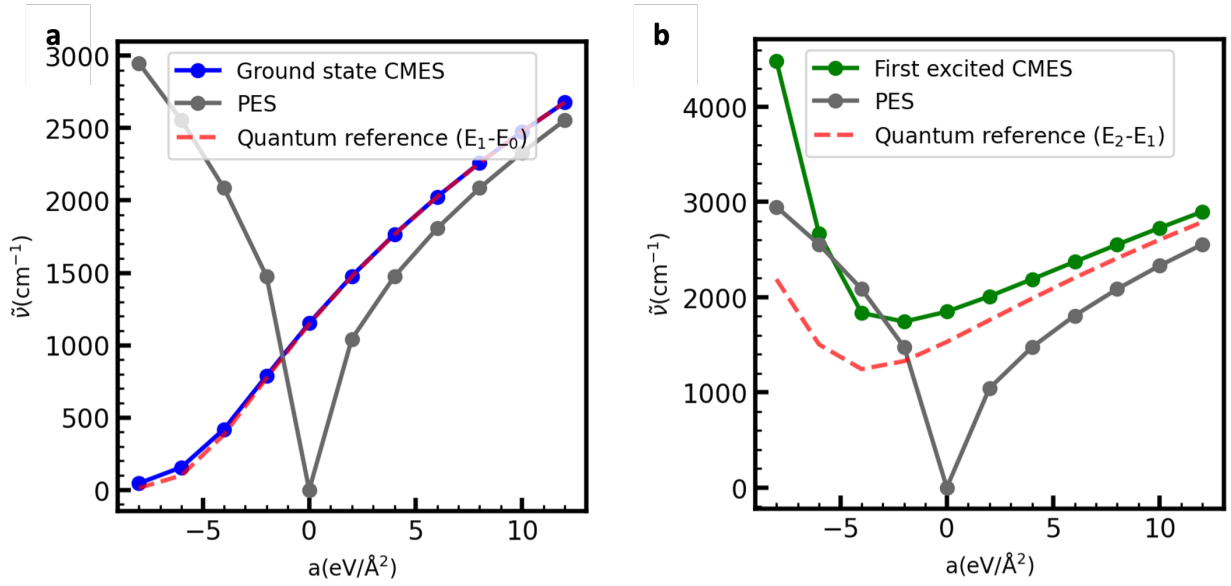

Figure 5: Transition frequencies from harmonic approximations using CMESs (colored solid line) and PES (grey solid line) for model potential $V(x) = ax^2 + bx^4$ for (**a**) the $0 \rightarrow 1$ transition and (**b**) the $1 \rightarrow 2$ transition. The parameter b is fixed to 32eV/Å^4 and a is allowed to vary. Our CMES-based method outperforms the conventional PES-based method with much better qualitative agreement with the quantum reference.

be used to describe vibrational excited states absorptions.

The studies in this paper are all proof-of-principle model system tests, in which we have assumed the underlying PES is known and build ground and excited state CMES on top of it. However, this procedure is not practical for real systems because obtaining PES is already computational highly demanding and constructing CMES is even more challenging. Fortunately, similar to the ground state CMES, which can be obtained from CNEO-DFT calculations, we anticipate that excited states CMESs can be calculated with excited states CNEO methods, for example, CNEO time-dependent density functional theory (CNEO-TDDFT). The related method development on CNEO-TDDFT for real molecules is ongoing in our group, and this current paper on model systems serves as the theoretical motivation for its development. All these developments will make CNEO method promising approaches for modeling and interpreting vibrational spectra for a variety of vibrational spectroscopy.

Acknowledgment

We thank Nan Yang and Yuzhe Zhang for helpful discussions. The authors are grateful for the funding support from the National Science Foundation under Grant 2238473 and from the University of Wisconsin via the Wisconsin Alumni Research Foundation.

References

(1) Perakis, F.; De Marco, L.; Shalit, A.; Tang, F.; Kann, Z. R.; KuÌhne, T. D.; Torre, R.; Bonn, M.; Nagata, Y. Vibrational spectroscopy and dynamics of water. *Chemical reviews* **2016**, *116*, 7590–7607.

(2) Wolke, C. T.; Fournier, J. A.; Dzugan, L. C.; Fagiani, M. R.; Odbadrakh, T. T.; Knorke, H.; Jordan, K. D.; McCoy, A. B.; Asmis, K. R.; Johnson, M. A. Spectroscopic snapshots of the proton-transfer mechanism in water. *Science* **2016**, *354*, 1131–1135.

(3) Yang, N.; Duong, C. H.; Kelleher, P. J.; McCoy, A. B.; Johnson, M. A. Deconstructing waterâs diffuse OH stretching vibrational spectrum with cold clusters. *Science* **2019**, *364*, 275–278.

(4) Ashihara, S.; Huse, N.; Espagne, A.; Nibbering, E. T.; Elsaesser, T. Vibrational couplings and ultrafast relaxation of the O–H bending mode in liquid H2O. *Chemical physics letters* **2006**, *424*, 66–70.

(5) Garrett-Roe, S.; Perakis, F.; Rao, F.; Hamm, P. Three-dimensional infrared spectroscopy of isotope-substituted liquid water reveals heterogeneous dynamics. *The Journal of Physical Chemistry B* **2011**, *115*, 6976–6984.

(6) Dong, P.-T.; Cheng, J.-X. Pump–probe microscopy: theory, instrumentation, and applications. *Spectroscopy* **2017**, *32*, 24–36.

(7) Hamm, P.; Zanni, M. *Concepts and methods of 2D infrared spectroscopy*; Cambridge University Press, 2011.

(8) Khalil, M.; Demirdöven, N.; Tokmakoff, A. Coherent 2D IR spectroscopy: Molecular structure and dynamics in solution. *The Journal of Physical Chemistry A* **2003**, *107*, 5258–5279.

(9) Petti, M. K.; Lomont, J. P.; Maj, M.; Zanni, M. T. Two-dimensional spectroscopy is being used to address core scientific questions in biology and materials science. *The Journal of Physical Chemistry B* **2018**, *122*, 1771–1780.

(10) Barone, V. Vibrational zero-point energies and thermodynamic functions beyond the harmonic approximation. *The Journal of chemical physics* **2004**, *120*, 3059–3065.

(11) Barone, V. Anharmonic vibrational properties by a fully automated second-order perturbative approach. *The Journal of chemical physics* **2005**, *122*, 014108.

(12) Barone, V.; Biczysko, M.; Bloino, J. Fully anharmonic IR and Raman spectra of medium-size molecular systems: accuracy and interpretation. *Physical Chemistry Chemical Physics* **2014**, *16*, 1759–1787.

(13) Bowman, J. M. Self-consistent field energies and wavefunctions for coupled oscillators. *The Journal of Chemical Physics* **1978**, *68*, 608–610.

(14) Bowman, J. M. The self-consistent-field approach to polyatomic vibrations. *Accounts of Chemical Research* **1986**, *19*, 202–208.

(15) Iftimie, R.; Minary, P.; Tuckerman, M. E. Ab initio molecular dynamics: Concepts, recent developments, and future trends. *Proceedings of the National Academy of Sciences* **2005**, *102*, 6654–6659.

(16) Tuckerman, M. E.; Martyna, G. J. Understanding modern molecular dynamics: Techniques and applications. 2000.

(17) Tuckerman, M. E. Ab initio molecular dynamics: basic concepts, current trends and novel applications. *Journal of Physics: Condensed Matter* **2002**, *14*, R1297.

(18) Iftimie, R.; Minary, P.; Tuckerman, M. E. Ab initio molecular dynamics: Concepts, recent developments, and future trends. *Proceedings of the National Academy of Sciences* **2005**, *102*, 6654–6659.

(19) Noid, D.; Koszykowski, M.; Marcus, R. A spectral analysis method of obtaining molecular spectra from classical trajectories. *The Journal of Chemical Physics* **1977**, *67*, 404–408.

(20) Swimm, R.; Delos, J. Semiclassical calculations of vibrational energy levels for nonseparable systems using the Birkhoff–Gustavson normal form. *The Journal of Chemical Physics* **1979**, *71*, 1706–1717.

(21) Yamada, T.; Aida, M. Fundamental absorption frequencies and mean structures at vibrational ground state from quasi-classical direct ab initio MD: Triatomic molecule. *Chemical Physics Letters* **2008**, *452*, 315–320.

(22) Yamada, T.; Aida, M. Structures of molecules in ground and excited vibrational states from quasiclassical direct ab initio molecular dynamics. *The Journal of Physical Chemistry A* **2010**, *114*, 6273–6283.

(23) Brieuc, F.; Bronstein, Y.; Dammak, H.; Depondt, P.; Finocchi, F.; Hayoun, M. Zero-point energy leakage in quantum thermal bath molecular dynamics simulations. *Journal of chemical theory and computation* **2016**, *12*, 5688–5697.

(24) Guo, Y.; Thompson, D. L.; Sewell, T. D. Analysis of the zero-point energy problem in classical trajectory simulations. *The Journal of chemical physics* **1996**, *104*, 576–582.

(25) Lu, D.-h.; Hase, W. L. Classical mechanics of intramolecular vibrational energy flow

in benzene. IV. Models with reduced dimensionality. *The Journal of chemical physics* **1988**, *89*, 6723–6735.

(26) Cao, J.; Voth, G. A. The formulation of quantum statistical mechanics based on the Feynman path centroid density. II. Dynamical properties. *The Journal of chemical physics* **1994**, *100*, 5106–5117.

(27) Jang, S.; Voth, G. A. A derivation of centroid molecular dynamics and other approximate time evolution methods for path integral centroid variables. *The Journal of chemical physics* **1999**, *111*, 2371–2384.

(28) Craig, I. R.; Manolopoulos, D. E. Quantum statistics and classical mechanics: Real time correlation functions from ring polymer molecular dynamics. *The Journal of chemical physics* **2004**, *121*, 3368–3373.

(29) Rossi, M.; Ceriotti, M.; Manolopoulos, D. E. How to remove the spurious resonances from ring polymer molecular dynamics. *The Journal of chemical physics* **2014**, *140*, 234116.

(30) Trenins, G.; Willatt, M. J.; Althorpe, S. C. Path-integral dynamics of water using curvilinear centroids. *The Journal of Chemical Physics* **2019**, *151*, 054109.

(31) Beck, M. H.; Jäckle, A.; Worth, G. A.; Meyer, H.-D. The multiconfiguration time-dependent Hartree (MCTDH) method: a highly efficient algorithm for propagating wavepackets. *Physics reports* **2000**, *324*, 1–105.

(32) Chen, Z.; Yang, Y. Incorporating Nuclear Quantum Effects in Molecular Dynamics with a Constrained Minimized Energy Surface. *The Journal of Physical Chemistry Letters* **2023**, *14*, 279–286.

(33) Xu, X.; Yang, Y. Constrained nuclear-electronic orbital density functional theory: En-

ergy surfaces with nuclear quantum effects. *The Journal of Chemical Physics* **2020**, *152*, 084107.

(34) Xu, X.; Yang, Y. Full-quantum descriptions of molecular systems from constrained nuclear–electronic orbital density functional theory. *The Journal of Chemical Physics* **2020**, *153*, 074106.

(35) Xu, X.; Yang, Y. Molecular vibrational frequencies from analytic Hessian of constrained nuclear–electronic orbital density functional theory. *The Journal of Chemical Physics* **2021**, *154*, 244110.

(36) Xu, X.; Chen, Z.; Yang, Y. Molecular dynamics with constrained nuclear electronic orbital density functional theory: Accurate vibrational spectra from efficient incorporation of nuclear quantum effects. *Journal of the American Chemical Society* **2022**, *144*, 4039–4046.

(37) Corcelli, S.; Lawrence, C.; Skinner, J. Combined electronic structure/molecular dynamics approach for ultrafast infrared spectroscopy of dilute HOD in liquid H 2 O and D 2 O. *The Journal of Chemical Physics* **2004**, *120*, 8107–8117.

(38) Li, F.; Skinner, J. Infrared and Raman line shapes for ice Ih. I. Dilute HOD in H 2 O and D 2 O. *The Journal of chemical physics* **2010**, *132*, 204505.

(39) Schmidt, J.; Roberts, S.; Loparo, J.; Tokmakoff, A.; Fayer, M.; Skinner, J. Are water simulation models consistent with steady-state and ultrafast vibrational spectroscopy experiments? *Chemical Physics* **2007**, *341*, 143–157.

(40) Auer, B.; Kumar, R.; Schmidt, J.; Skinner, J. Hydrogen bonding and Raman, IR, and 2D-IR spectroscopy of dilute HOD in liquid D2O. *Proceedings of the National Academy of Sciences* **2007**, *104*, 14215–14220.

(41) Schmidt, J.; Corcelli, S.; Skinner, J. Pronounced non-Condon effects in the ultrafast infrared spectroscopy of water. *The Journal of chemical physics* **2005**, *123*, 044513.

(42) Tuckerman, M. *Statistical mechanics: theory and molecular simulation*; Oxford university press, 2010.

(43) Huber, K.-P. *Molecular spectra and molecular structure: IV. Constants of diatomic molecules*; Springer Science & Business Media, 2013.